ACS OMEGA

Article

Cite This: ACS Omega 2017, 2, 9109−9117

pH-Regulated Synthesis of Trypsin-Templated Copper Nanoclusters with Blue and Yellow Fluorescent Emission

Jie Feng,[†] Yonglei Chen,*[,†] Yangxia Han,[†] Juanjuan Liu,[†] Sudai Ma,[†] Huige Zhang,[†] and Xingguo Chen*[,†,‡]

[†]State Key Laboratory of Applied Organic Chemistry and Department of Chemistry and [‡]Key Laboratory of Nonferrous Metal Chemistry and Resources Utilization of Gansu Province, Lanzhou University, Lanzhou 730000, China

Supporting Information

ABSTRACT: In this article, a simple protocol to prepare water-soluble fluorescent copper nanoclusters (CuNCs) using trypsin as a stabilizer and hydrazine hydrate as a reducing agent was reported. It was found that the pH of the reaction solution was critical in determining the fluorescence of CuNCs. CuNCs with blue and yellow fluorescent emission were obtained under basic and acidic conditions, respectively. Although the detailed formation mechanisms of these CuNCs required further analysis, the synthetic route was promising for preparing different fluorescent metal NCs for applications. With good water solubility and excellent photostability, the yellow-emitting CuNCs could serve as a fluorescence probe for detection of Hg^{2+} based on the aggregation-induced quenching mechanism. The fluorescence quenching efficiency had fantastic linearity to Hg^{2+} concentrations in the range of 0.1−100 μM, with a limit of detection of 30 nM. Additionally, the yellow-emitting CuNCs exhibited negligible cytotoxicity and were successfully applied to bioimaging of HeLa cells.

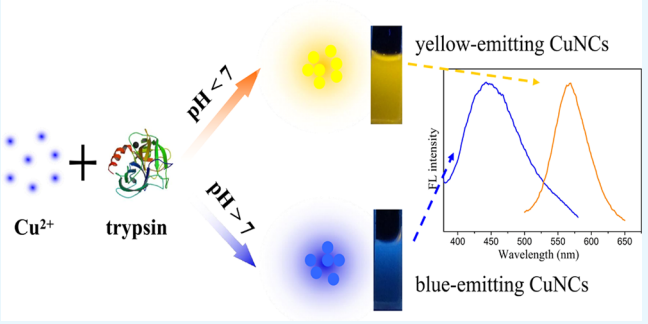

INTRODUCTION

Metal nanoclusters (MNCs), consisted of several to hundreds of metal atoms, have drawn considerable attention due to their unique physical, chemical, and optical properties resulting from their discrete energy levels and band-gap energy structures.[1,2] In particular, compared with conventional organic fluorophores and semiconductor quantum dots, fluorescent MNCs exhibit several advantages such as strong photoluminescence, good biocompatibility, excellent photostability, and sub-nanometer size.[3] Thus, they have been developed to be used in a wide range of applications in sensing[4,5] and imaging.[6,7]

Among the studied MNCs, gold NCs (AuNCs) and silver NCs (AgNCs) have received extensive research attention by size-controlled synthesis, structural characterization, and property investigations. In fact, compared with gold and silver, copper was more popular in industry because of its high conductivity and much lower cost. Nevertheless, over the past decades, studies on the synthesis, properties, and applications of copper NCs (CuNCs) were scarce primarily because of their susceptibility to oxidation and the difficulty in preparing extremely tiny particles.[8] In recent years, considerable efforts have been devoted to exploring the synthesis of fluorescent CuNCs and great progress has been achieved. By employing a series of scaffolds or capping agents, such as small molecules,[9] polymers,[10] oligonucleotides,[11] peptides,[12] and proteins,[13] stable CuNCs have been successfully prepared. Among these methods, protein-templated synthesis is particularly attractive as proteins could serve as environmentally benign reducing and stabilizing molecules. However, there were few reports on the discussion of the mechanism for the formation of CuNCs and it remained unclear how the protein template affected the CuNC fluorescence behaviors under various reaction conditions. In a previous report, the pH-dependent synthesis of pepsin−AuNCs with different fluorescent emission was developed. The different charges on pepsin under different pH conditions affected the structure of pepsin chains, which led to the formation of AuNCs with different fluorescent emission.[14] Therefore, it enlightened us whether multicolored CuNCs could be prepared by regulating the reaction pH.

Hg^{2+} is one of the most toxic heavy-metal ion pollutants that exists in water, soil, and food. Mercury can accumulate in organisms and has long-term adverse effects on liver, kidney, central nervous system, and so on. Therefore, developing effective methods for the sensitive and selective detection of Hg^{2+} was especially important for environmental monitoring and clinical research. Traditional methods of Hg^{2+} sensing, including atomic absorption/emission spectroscopy, inductively coupled plasma mass spectrometry, stripping voltammetry, etc.[15−18] were limited by the disadvantages of requiring expensive instruments, the complex procedures in sample preparation, a specific worker, etc. Electrochemical, colorimetric, and fluorescent sensors for Hg^{2+} have also been

Received: July 24, 2017
Accepted: November 30, 2017
Published: December 19, 2017

DOI: 10.1021/acsomega.7b01052
ACS Omega 2017, 2, 9109−9117

Scheme 1. Illustration of the Synthesis of CuNCs with Blue and Yellow Emission

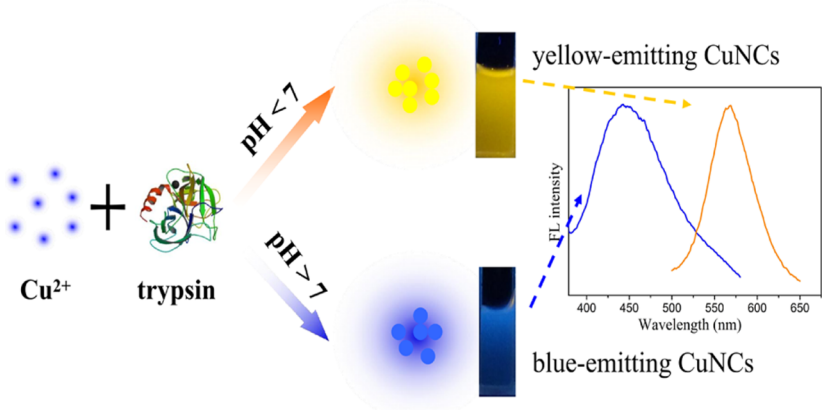

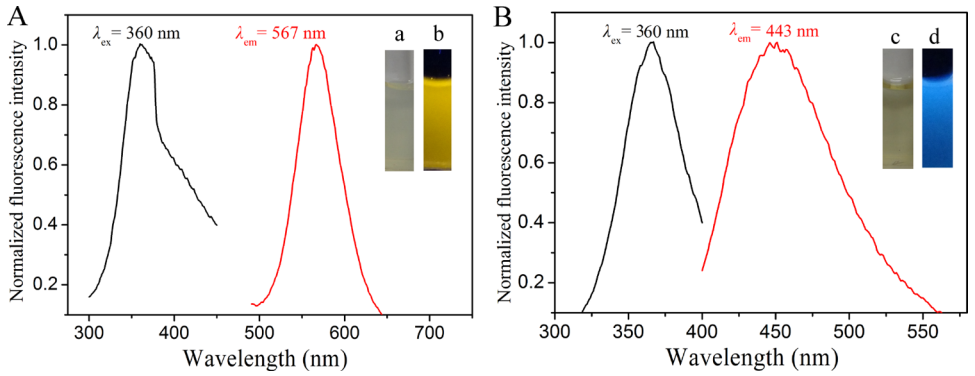

Figure 1. Fluorescence excitation and emission spectra of the yellow- (A) and blue- (B) emitting CuNCs; insets show photographs of the CuNC solution under visible (a, c) and UV (b, d) light irradiation.

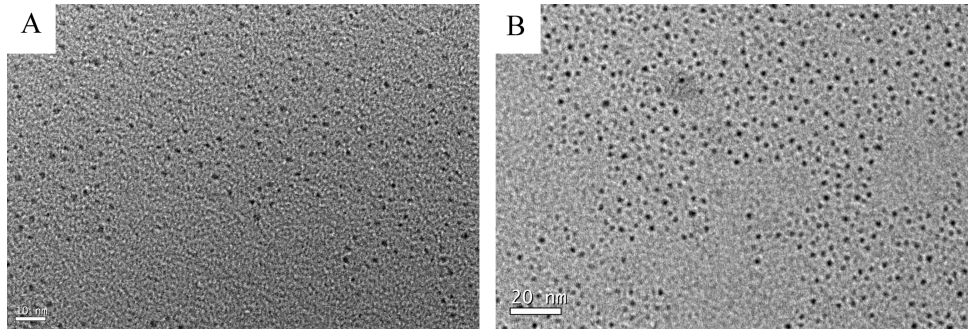

Figure 2. TEM images of the blue-emitting (A) and yellow-emitting (B) CuNCs.

reported over the past decade.[19−29] Among these methods, fluorescent Hg^{2+} sensors based on various nanoparticles have been developed due to their unique advantages such as high sensitivity, simple operation, and fast response.[30−33]

On the basis of the above conditions, we reported for the first time a pH-dependent synthesis of CuNCs with blue and yellow fluorescent emission using trypsin as a template and hydrazine hydrate as a reducing agent (Scheme 1). Trypsin is an important digestive enzyme produced by pancreatic acinar cells.[34] It is also a good candidate for synthesis of trypsin-stabilized CuNCs as trypsin is rich in amino acid residues, with 7 cysteine (Cys) and 10 tyrosine (Tyr) residues. The different conformational states of the trypsin molecule under different pH conditions could affect the interaction between trypsin and copper ion surface, leading to the formation of CuNCs with different sizes at different pH conditions. Then, the prepared yellow-emitting CuNCs were successfully employed as an effective fluorescent probe for Hg^{2+} sensing. Because of the low toxicity and good biocompatibility of the yellow-emitting CuNCs, they were also used in cell labeling of HeLa cells.

RESULTS AND DISCUSSION

Trypsin contained rich Cys, His, and Tyr that could act as chelating groups for sequestering copper ions and polyvalent ligands for passivating the surface of metallic materials.[35] Next, the reducing agent N_2H_4 was applied to quickly reduce Cu^{2+} cations to CuNCs. It has been reported that proteins exhibit different conformational states at different pH levels, which could affect the size and fluorescence properties of MNCs.[14] Therefore, it was of interest to investigate the synthesis of trypsin-templated CuNCs at different pH values. In a typical synthesis, trypsin and $CuSO_4$ solution was mixed thoroughly.

DOI: 10.1021/acsomega.7b01052
ACS Omega 2017, 2, 9109−9117

For the synthesis of yellow- and blue-emitting CuNCs, the pH of the mixture was adjusted to 3.4 and 12.0, respectively, before addition of N_2H_4. It was worth noting that after addition of N_2H_4 to the mixture, the solution pH changed from 3.4 to 5.1 for the yellow-emitting CuNCs and remained unchanged for the blue-emitting CuNCs. After incubating at 70 °C for 2 h, CuNCs with different fluorescent emission were obtained. Figure 1 shows the maximum fluorescence excitation and emission peaks of the prepared CuNCs. The diluted yellow- and blue-emitting CuNC solutions were nearly colorless (or very pale yellow) and transparent under visible light, whereas they exhibited yellow and blue fluorescence under UV light irradiation (365 nm), respectively (inset of Figure 1). As shown in Figure S1A, the emission wavelength of blue-emitting CuNCs was red-shifted from 415 to 475 nm with the excitation wavelength ranging from 310 to 400 nm, whereas the emission wavelength was almost independent of the excitation wavelength for the yellow-emitting CuNCs (Figure S1B). The difference of the fluorescence behaviors may be caused by the different surface states of the CuNCs with blue and yellow emission. The absolute quantum yields (QYs) for the CuNCs in aqueous solutions were measured as 3.1 and 0.1% for yellow and blue emission, respectively. The morphology and size of CuNCs were clearly revealed by transmission electron microscopy (TEM) images. Figure 2 shows that CuNCs were highly uniform and monodisperse. The average diameters of CuNCs for blue and yellow emission were about 1.8 and 2.5 nm, respectively. These results were highly in accord with the phenomenon of fluorescence wavelength dependence on the size of CuNCs. That is, the larger size of CuNCs corresponded to the red-shifted fluorescence emission wavelength, similar to that for other fluorescent nanostructures such as AuNCs.[36] Figure S2 shows the UV−vis absorption spectra of the as-prepared CuNCs and trypsin. The absorption spectrum of trypsin had a peak centered at 276 nm, and it was changed when CuNCs were formed. The rather broad spectra with a small red-shifted hump confirmed the formation of CuNCs. Furthermore, there was no apparent surface plasmon resonance absorption band appearing at around 560−600 nm, indicating no large copper nanoparticles in the CuNC samples.[37,38] The slight blue shift of the absorption for the blue-emitting CuNCs compared to that of the yellow-emitting CuNCs further confirmed that the blue-emitting CuNCs were smaller in size than that of the yellow-emitting CuNCs.[39]

In most reports, MNCs synthesized with the assistance of proteins were generally prepared under basic pH conditions.[40−44] It was mainly because proteins possessed good reducing capacity when the reaction pH was greater than pK_a of Tyr (~10)[44] and it could act as a reductant. However, in the present study, yellow-emitting CuNCs were obtained when the synthesis was conducted at pH 3.4. Although it was unclear how trypsin "biomineralized" fluorescent CuNCs, the present results clearly showed that the pH of the reaction solution played an important role in the determination of CuNCs with yellow and blue fluorescent emission. Far-UV circular dichroism (CD) spectra of the trypsin solution at different pH values were recorded to investigate the mechanism of pH-dependent formation of multicolored CuNCs. As shown in Figure 3, compared to that for the trypsin at pH 12.0, a negative band at around 198 nm from the random coil became more predominant for the trypsin at pH 3.4. It indicated that a large conformational change for trypsin occurred because of the denaturation of trypsin under acidic pH conditions. More

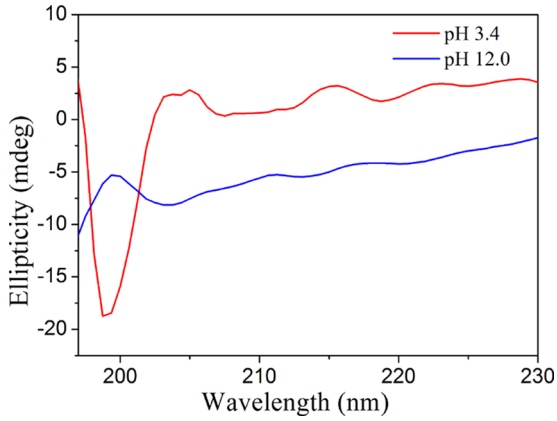

Figure 3. CD spectra of the aqueous solution of trypsin at different pHs.

functional groups, such as −OH, −NH, and −COOH, could thus be accessible to interact with copper, and large internal spaces within the weak-bonding random-coiled trypsin may be utilized for the formation of large CuNCs. Accordingly, it was concluded that different secondary structures of trypsin at different pH levels could affect the formation of CuNCs with different sizes. Fourier transform infrared (FT-IR) spectra is an excellent tool for the structural characterization of proteins in various environments. It has been reported that the amide I band in the FT-IR spectrum was also sensitive to the change of protein secondary structure.[45] Figure S3 revealed that the characteristic vibration peaks of trypsin were unaltered after the blue-emitting CuNCs formed, whereas an obvious shift of the amide I band to lower wavenumbers was observed after the formation of yellow-emitting CuNCs. This indicated that a conformational change for the trypsin of yellow-emitting CuNCs occurred under acidic pH conditions. Therefore, all of these results confirmed that the mechanism for the formation of pH-dependent multicolored CuNCs was based on the changes of the secondary structure of trypsin at different pH levels.

In the present study, as the yellow-emitting CuNCs possessed good water solubility and strong fluorescence intensity, they could be explored as a fluorescent probe for practical sensing. To improve the sensitivity of the fluorescent probe, several experimental conditions including the concentration, temperature, and reaction time were optimized to obtain yellow-emitting CuNCs with high fluorescence intensity. In this method, we found that N_2H_4 was necessary in the preparation of CuNCs. As shown in Figure S4, in the preparation of yellow-emitting CuNCs, the product synthesized in the absence of N_2H_4 exhibited no fluorescence signal. From this phenomenon, it could be concluded that trypsin alone was not enough to reduce Cu ions. N_2H_4 was deemed as a reducing agent. In addition to N_2H_4, several other reducing agents such as ascorbate and $NaBH_4$ were also applied for the synthesis of yellow-emitting CuNCs. As shown in Figure S5, the CuNCs with N_2H_4 as the reducing agent exhibited relatively strong fluorescence intensity. The fluorescence spectra of the CuNCs prepared with different molar ratios of $CuSO_4$ and N_2H_4 (keeping the concentration of trypsin constant) are shown in Figure S6A. It could be seen that the product with a molar ratio of 1:1 exhibited the maximum fluorescence intensity at 567 nm. The reaction temperature was also investigated in the synthesis of fluorescent CuNCs. As shown in Figure S6B, external heat

DOI: 10.1021/acsomega.7b01052
ACS Omega 2017, 2, 9109−9117

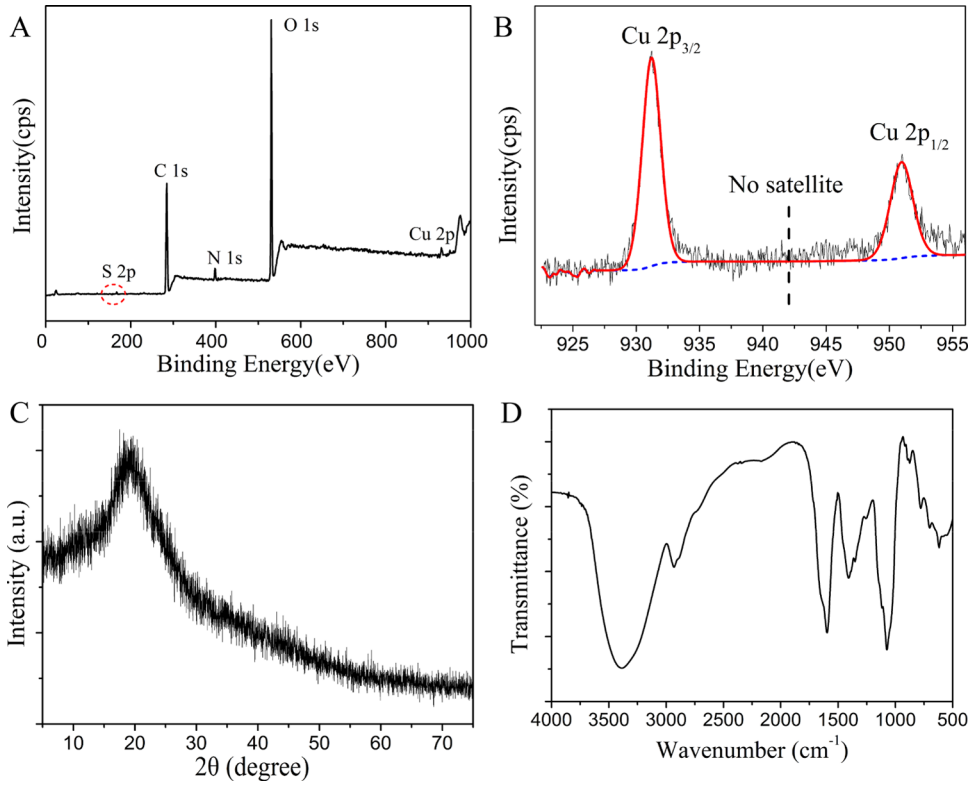

Figure 4. (A) XPS full-scan spectrum of CuNCs. (B) High-resolution XPS spectrum of the Cu 2p peak of CuNCs. (C) Powder XRD pattern of CuNCs. (D) FT-IR spectrum of yellow-emitting CuNCs.

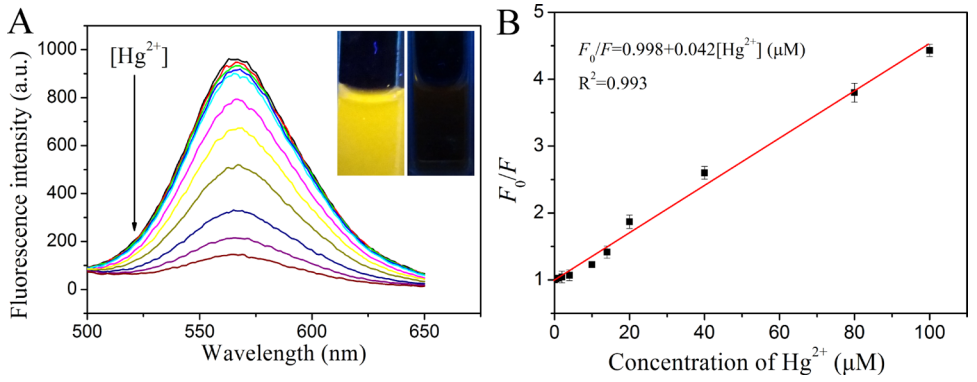

Figure 5. (A) Fluorescence emission spectra of CuNCs upon addition of various concentrations of Hg^{2+}. The insets show the photographs of CuNC solutions in the absence and presence of 100 μM Hg^{2+} under UV light (365 nm). (B) Relationship between F_0/F and the concentration of Hg^{2+} in the range of 0.1−100 μM.

could significantly accelerate the generation of CuNCs; thus, 70 °C was chosen as the reaction temperature. Under these reaction conditions, the fluorescence intensity reached maximum with the reaction time up to 2.0 h, and after that, it decreased (Figure S6C). This result might be attributed to the redistribution or interprotein transfer of copper ions after 2.0 h.[46] Therefore, an optimum reaction time of 2.0 h was used in the whole study. Therefore, the yellow-emitting CuNCs prepared under optimal synthetic conditions were used for conducting the following research.

It was well known that Cu was easily oxidized because of its low reduction potential. Therefore, it was important to confirm the oxidation state of Cu in the CuNC sample. An X-ray photoelectron spectroscopy (XPS) survey spectrum showed that the sample was composed of all of the expected elements C, N, O, S, and Cu (Figure 4A). The high-resolution XPS spectrum of the Cu 2p peak of CuNCs is displayed in Figure 4B. Two intense peaks at 951.0 and 931.2 eV were assigned to the binding energies of Cu $2p_{1/2}$ and $2p_{3/2}$ from Cu(0), and the result was consistent with the previous report.[9,41] In addition, no characteristic satellite peak at around 942 eV implied the absence of Cu^{2+} in CuNCs. This thus precluded any significant oxidation of CuNCs.[47] Nevertheless, it was known that the typical $2p_{3/2}$ binding energy of Cu(0) was only ∼0.1 eV away from that of the Cu(I) species.[8] Therefore, the valence state of Cu in our samples likely lied between 0 and +1. The powder X-ray diffraction (XRD) pattern of CuNCs showed a broad peak at around 20° (Figure 4C). The result supported the absence of a significant population of crystalline Cu nanoparticles in the sample.[48] Next, the surface bonds of the synthesized CuNCs

DOI: 10.1021/acsomega.7b01052
ACS Omega 2017, 2, 9109−9117

Table 1. Comparison of the Sensing Performance of Different Fluorescent Probes for Hg^{2+} Detection

sensing material	linear range (μM)	LOD (nM)	response time (min)	reference
nitrogen-doped carbon quantum dots	0−25	230		49
trypsin-stabilized AuNCs	0.05−0.6	50		50
β-lactoglobulin-stabilized AuNCs	0.05−500	30	2	51
BSA−AuAg BNCs	0.05−6.3	13	5	52
DNA duplex-templated AgNCs	0.01−0.3	10	>60	53
oligonucleotide-stabilized AgNCs	0.005−1.5	5	3	54
DNA-templated AgNCs	0.0025−0.05	0.9	30	55
CuNCs	0.1−100	30	2	this work

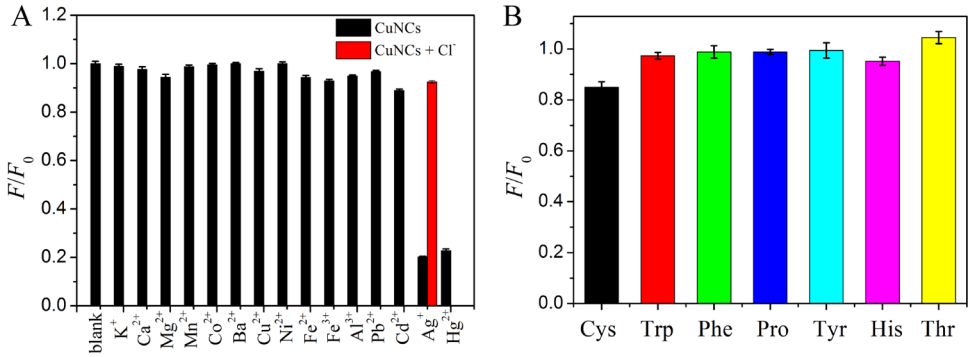

Figure 6. Selectivity of the CuNC sensor toward Hg^{2+} over other metal ions (A) and amino acids (B). The concentrations of Hg^{2+} and interfering substances were 100 and 500 μM, respectively. The concentration of Cl^- was 2 mM.

were analyzed by FT-IR. As shown in Figure 4D, the peaks at 3400−3000 cm^{-1} due to −NH and −OH stretching vibrations were also prominent in the spectra, indicating the existence of free $-NH_2$/−COOH groups in CuNCs.

To test the feasibility of using the as-prepared CuNCs in practical sensing applications, the stability of the CuNC probe was investigated. As shown in Figure S7, both the blue- and yellow-emitting CuNCs were observed to be very stable that the fluorescence intensity had no change under continuous light irradiation for 60 min. In addition, CuNCs displayed relatively stable fluorescence intensities even under extreme pH conditions (Figure S8). From Figure S9, it could be noted that the fluorescence intensity remained nearly constant when the concentration of NaCl was as high as 50 mM. These results indicated that the as-prepared CuNCs had excellent photostability and salt tolerance.

In this work, it was observed that the fluorescence intensity of the yellow-emitting CuNCs was sensitively quenched in the presence of Hg^{2+}. As demonstrated in Figure 5A, with the addition of different concentrations of Hg^{2+}, the fluorescence intensity of the CuNC solution decreased proportionately. The fluorescence response was rapid, and the reaction completely achieved a balance within 1 min (Figure S10). To achieve maximum quenching efficiency, the type of buffer solution and detection pH value have been optimized. As shown in Figure S11A, CuNCs exhibited strongest fluorescence intensity in the pH 4.0 phosphate-buffered saline (PBS) buffer solution compared to that in other buffer solutions. In addition, with the addition of Hg^{2+} to the CuNC solution, the fluorescence quenching efficiency reached maximum in the pH 4.0 PBS buffer solution (Figure S11B). Therefore, the pH 4.0 PBS buffer solution was selected for detection of Hg^{2+}. Under optimum conditions, the quenching efficiency (F_0/F) displayed a good linear relationship (R^2 = 0.993) with the concentration of Hg^{2+} ranging from 0.1 to 100 μM, where F_0 and F are the fluorescence intensities of the CuNC solution in the absence and presence of Hg^{2+}, respectively. The limit of detection (LOD) ($3s/k$, in which s is the standard deviation for the control and k is the slope of the calibration curve) was estimated to be 30 nM, which was lower or comparable to that obtained by other fluorescent probes for Hg^{2+} sensing (Table 1).[49−52] It should be noted that the sensitivity of the CuNC sensor for Hg^{2+} was lower than that of DNA-templated fluorescence nanoclusters.[53−55] Nevertheless, the proposed method in this work was much easy-going and time-saving, which made it more convenient for practical applications.

Besides those of Hg^{2+}, the effects of some other metal ions and several amino acids on the assay system were further investigated under the same test conditions. As shown in Figure 6, the fluorescence intensity of CuNCs decreased significantly by adding Hg^{2+} to the solution, whereas other metal ions (K^+, Ca^{2+}, Mg^{2+}, Mn^{2+}, Co^{2+}, Ba^{2+}, Cu^{2+}, Ni^{2+}, Fe^{2+}, Fe^{3+}, Al^{3+}, Cd^{2+}, and Pb^{2+}) and several amino acids (Cys, Trp, Pro, Tyr, His, Thr, Phe) had only a slight or negligible effect on the fluorescence intensity, even when the concentration of the potential interferences was 5-fold higher than that of Hg^{2+}. It is worth mentioning that other than Hg^{2+}, Ag^+ ions also led to great decreases in the fluorescence intensity. To eliminate the interference, a chelating ligand, sodium chloride (2.0 mM), which showed effective masking ability for Ag^+, was added to the solution. As a result, even in the presence of Ag^+ at a concentration 5 times greater than that of Hg^{2+}, no obvious fluorescence quenching was observed, thus exhibiting improved selectivity of the CuNC probe toward Hg^{2+}. The results demonstrated that the fluorescent CuNC probe exhibited excellent selectivity toward Hg^{2+}.

To date, several Hg^{2+}-induced fluorescence quenching mechanisms have been proposed. Morishita et al. noticed a significant quenching of AgNCs by Hg^{2+}, and they attributed it to the redox reaction mechanism.[56] In our present work, the

DOI: 10.1021/acsomega.7b01052
ACS Omega 2017, 2, 9109−9117

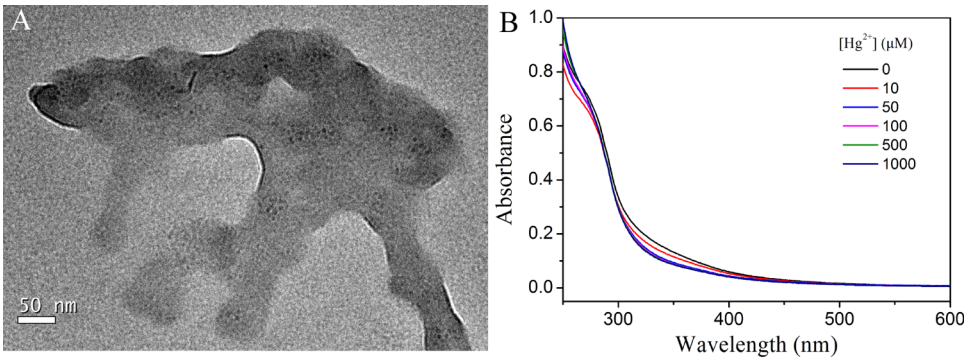

Figure 7. (A) TEM image of CuNCs after addition of Hg^{2+}. (B) UV−vis spectra of CuNCs before and after addition of different concentrations of Hg^{2+}.

oxidation state of Cu in CuNCs was investigated by the XPS spectra in the absence and presence of 100 μM Hg^{2+}, respectively. As shown in Figure S12, the addition of Hg^{2+} to the CuNC solution had little effect on the oxidation state of Cu, which ruled out the redox-reaction-induced CuNC fluorescence quenching. Other fluorescence quenching mechanisms could be taken into consideration. To study the Hg^{2+}-induced fluorescence quenching mechanism, the TEM image of CuNCs after addition of Hg^{2+} was investigated (Figure 7A). It was clear that CuNCs obviously aggregated after Hg^{2+} was added. As it was reported, Hg^{2+} has a strong affinity toward amino and carboxylic groups on the surface of CuNCs.[57,58] The interaction between Hg^{2+} and CuNCs made the CuNCs close to each other. Thus, fluorescence quenching of CuNCs was ascribed to the aggregation of CuNCs induced by Hg^{2+}, thus facilitating the efficient energy transfer. The phenomenon was consistent with the previous report by Huang.[59] In addition, the fact that quenching by Hg^{2+} did not affect markedly either the fluorescence emission spectrum or the absorption spectrum of CuNCs (Figure 7B) further indicated the quenching mechanism of energy transfer between CuNCs and Hg^{2+}.[60]

The practical application of this fluorescence method was evaluated through the detection of Hg^{2+} in human urine and serum samples. Three concentrations of Hg^{2+} were spiked into the samples. The recovery values were in the range of 89.0−105.0 and 95.0−108.8% in urine and serum samples, respectively (Table 2). These results demonstrated that the current strategy for Hg^{2+} sensing in practical samples was reliable and feasible.

Table 2. Analytical Results for the Detection of Hg^{2+} Ions in Different Natural Samples by the Proposed Method[a]

	urine		serum	
spiked concentration (μM)	found (μM)	recovery (%)	found (μM)	recovery (%)
4.0	4.2 ± 0.5	105.0	3.8 ± 0.4	95.0
20.0	17.8 ± 0.4	89.0	20.1 ± 0.8	100.5
40.0	37.3 ± 0.4	93.3	43.5 ± 0.3	108.8

[a] n = 3.

To apply the yellow-emitting CuNCs in the field of biological imaging, 3-(4,5-dimethylthiazol-2-yl)-2,5-diphenyltetrazolium bromide (MTT) assays were carried out to assess the cytotoxicity of the CuNC probes to HeLa cells. HeLa cells were incubated with various concentrations of CuNCs in standard cell culture conditions. After incubation for 24 h, the viability of the cells was determined. As shown in Figure 8, the cell viability was found to be greater than 82% even when the

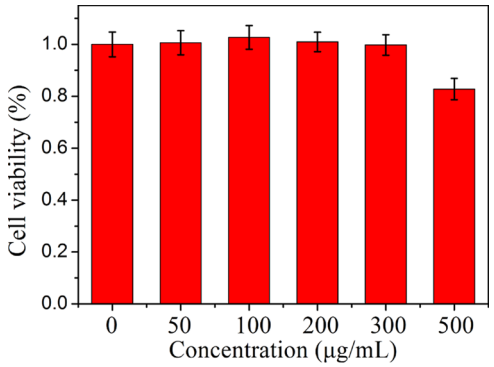

Figure 8. Cell viability of HeLa cells in the presence of different concentrations of CuNCs.

concentration of CuNCs was up to 500 μg/mL. High cell viability demonstrated the low toxicity and excellent biocompatibility of the as-prepared CuNCs, which made them suitable for cell imaging.

As shown in Figure 9, by incubating Hela cells with CuNCs (500 μg/mL) for 1 h at 37 °C, a significant yellow emission from the intracellular region could be observed. All of these results showed that the yellow-emitting CuNCs could be applied in the field of biological imaging and cell labeling.

CONCLUSIONS

In summary, CuNCs with yellow and blue fluorescent emission were synthesized with a facile approach in the presence of trypsin and N_2H_4. The pH of the reaction solution was critical in determining whether CuNCs showed yellow or blue fluorescent emission. As the yellow-emitting CuNCs exhibited excellent stability, low toxicity, and good biocompatibility, the fluorescent CuNCs were successfully used in not only the detection of Hg^{2+} but also cell imaging in HeLa cells. Therefore, this facile preparation of multicolored CuNCs offered access to promising candidates for biological labeling and sensing applications.

EXPERIMENTAL SECTION

Materials. Trypsin from bovine pancreas was obtained from Aladdin Co., Ltd (Shanghai, China). $CuSO_4{\cdot}5H_2O$ was purchased from Shanghai Bodi Chemical Co., Ltd (Shanghai, China). $HgCl_2$, KCl, $CaCl_2$, $MgCl_2$, $MnCl_2$, $CoCl_2$, $BaCl_2$,

DOI: 10.1021/acsomega.7b01052
ACS Omega 2017, 2, 9109−9117

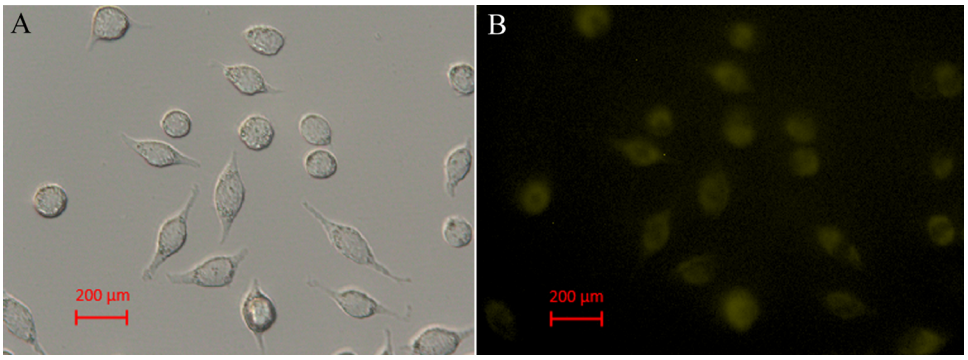

Figure 9. Fluorescence microscopy image (A) and its corresponding bright-field transmission image (B) of HeLa cells incubated with 500 μg/mL CuNCs for 1 h at 37 °C.

$CuCl_2$, $NiCl_2$, $FeCl_2$, $FeCl_3$, and $AlCl_3$ were purchased from Sinopharm Chemical Reagent Co., Ltd. (Shanghai, China). L-Tryptophan (L-Trp), L-proline (L-Pro), L-tyrosine (L-Tyr), L-histidine (L-His), L-threonine (L-Thr), and L-phenylalanine (L-Phe) were purchased from Shanghai Sangon Biotechnology Co., Ltd. (Shanghai, China).

pH-Dependent Synthesis of Copper Nanoclusters (CuNCs). All glassware was cleaned in a bath of freshly prepared 3:1 HCl/HNO_3 and rinsed thoroughly in water before use. Yellow-emitting CuNCs were prepared as follows. Typically, 1 mL of $CuSO_4$ solution (10 mM) was added to 1 mL of trypsin (40 mg/mL) under vigorous stirring at room temperature. Five minutes later, the pH of the obtained solution was about 3.4. Then, 100 μL of N_2H_4 solution (100 mM) was added dropwise under vigorous stirring. The reaction mixture was incubated at 70 °C in a water bath for 2 h, and the color changed gradually from light blue to pale yellow. After the reaction, CuNCs were purified by centrifuging at 12 000 rpm to remove large particles. The resultant yellow-emitting CuNCs were stored at 4 °C for further use.

To obtain the blue-emitting CuNCs, similar synthesis was conducted except that the pH of the solution before addition of N_2H_4 was adjusted to 12 by 1 M NaOH. The final dark brown solution of CuNCs exhibited a blue-emitting fluorescence under UV lamp irradiation.

Fluorescence Detection of Hg^{2+}. For the typical assay of Hg^{2+}, 300 μL of the prepared yellow-emitting CuNCs solution was added into 2.2 mL of the PBS buffer solution (pH 4.0, 10.0 mM) to prepare the probe solution. The solution (10.0 μL) with different concentrations of Hg^{2+} was added into the probe solution. Fluorescence emission spectra were collected with excitation at 360 nm after 60 s. In the selectivity experiment, a series of potential metal ions and amino acids were mixed with the probe solution. The concentrations of the these interferences were 500 μM.

Characterization. All of the instruments used for characterization were the same as those used in the previous work.[10,61] Transmission electron microscopy (TEM) images of CuNCs with different fluorescent emission were obtained using a Tecnai G2F30 instrument. Fourier transform infrared (FT-IR) spectra were recorded on a Nicolet Nexus 670 spectrometer using KBr pellets. Powder X-ray diffraction (XRD) patterns were recorded on a D/max 82400 X-ray powder diffractometer (Rigaku, Japan) with Cu Kα radiation (λ = 0.154056 Å). X-ray photoelectron spectroscopy (XPS) measurement was performed using a PerkinElmer PHI-5702 multifunctional photoelectron spectrometer equipped with an Al Kα exciting source. Far-UV circular dichroism (CD) spectra of trypsin under different pH conditions were recorded at 25 °C on an Olis DSM 1000 double-beam spectrophotometer. UV−visible absorption spectra were recorded by a TU-1901 double-beam UV−vis spectrophotometer. Fluorescence measurements were carried out using a RF-5301 spectrofluorophotometer with both excitation and emission slits set at 10.0 nm. The excitation wavelength was set at 360 nm. Samples for absorption and emission measurements were taken in 1 cm × 1 cm quartz cuvette. The absolute photoluminescence quantum yield (QY) of CuNCs was measured and calculated using an "Edinburgh Instruments" FLS 920 spectrometer, which has been reported by our previous work (see Supporting Information).[10]

MTT Assay. The human cervical carcinoma HeLa cells were cultured in RPMI-1640 medium supplemented with 10% fetal bovine serum using a 96-well culture plate and kept in an incubator at 37 °C with a humidified atmosphere of 5% CO_2. Prior to test, 1×10^4 cells were incubated in 96-well plates for 24 h at 37 °C in a final volume of 100 μL. Then, 10 μL of CuNCs with different concentrations (0, 50, 100, 200, 300, and 500 μg/mL, respectively) was added and incubated for another 24 h. Afterward, cells were rinsed twice with PBS (10 mM, pH 7.4) followed by addition of 100 μL of fresh medium and 10 μL of 3-(4,5-dimethylthiazol-2-yl)-2,5-diphenyltetrazolium bromide (MTT) (5 mg/mL) to each well. The cells were incubated for additional 4 h at 37 °C. After removing all medium from the wells, 100 μL of dimethylsulfoxide was added to each well and mixed thoroughly for 5 min. The optical density (OD) of the mixture was measured at 570 nm using a microplate reader. The cell viability was estimated as (OD treated/OD control) × 100%, where OD control and OD treated were obtained in the absence and presence of CuNCs, respectively.[62]

In Vivo Fluorescence Imaging. The HeLa cells were cultured in RPMI-1640 medium supplemented with 10% fetal bovine serum at 37 °C with 5% CO_2 overnight. Then, CuNCs (500 μg/mL) were added to the cell culture, and the cells were incubated for another 1 h at 37 °C. After the cells were washed with PBS three times, the fluorescence images were acquired by a fluorescent microscope.

■ ASSOCIATED CONTENT

Supporting Information

The Supporting Information is available free of charge on the ACS Publications website at DOI: 10.1021/acsomega.7b01052.

Details about the absolute QY and additional Figures (S1−S12) (PDF)

DOI: 10.1021/acsomega.7b01052
ACS Omega 2017, 2, 9109−9117

AUTHOR INFORMATION

Corresponding Authors

*E-mail: chyl@lzu.edu.cn. Tel: +86-931-8912763. Fax: +86-931-8912582 (Y.C.).

*E-mail: chenxg@lzu.edu.cn (X.C.).

ORCID

Xingguo Chen: 0000-0002-7982-1519

Notes

The authors declare no competing financial interest.

ACKNOWLEDGMENTS

The authors are grateful for financial support from the National Nature Science Foundation of China (No. 21675068).

REFERENCES

(1) Gittins, D. I.; Bethell, D.; Schiffrin, D. J.; Nichols, R. J. A nanometre-scale electronic switch consisting of a metal cluster and redox-addressable groups. *Nature* **2000**, *408*, 67−69.

(2) Luo, Z.; Zheng, K.; Xie, J. Engineering ultrasmall water-soluble gold and silver nanoclusters for biomedical applications. *Chem. Commun.* **2014**, *50*, 5143−5155.

(3) Zhang, L.; Wang, E. Metal nanoclusters: New fluorescent probes for sensors and bioimaging. *Nano Today* **2014**, *9*, 132−157.

(4) Shojaeifard, Z.; Hemmateenejad, B.; Shamsipur, M. Efficient on-off ratiometric fluorescence probe for cyanide ion based on perturbation of the interaction between gold nanoclusters and a copper(II)-phthalocyanine complex. *ACS Appl. Mater. Interfaces* **2016**, *8*, 15177−15186.

(5) Wang, C.; Lin, H.; Xu, Z.; Huang, Y.; Humphrey, M. G.; Zhang, C. Tunable carbon-dot-based dual-emission fluorescent nanohybrids for ratiometric optical thermometry in living cells. *ACS Appl. Mater. Interfaces* **2016**, *8*, 6621−6628.

(6) Venkatesh, V.; Shukla, A.; Sivakumar, S.; Verma, S. Purine-stabilized green fluorescent gold nanoclusters for cell nuclei imaging applications. *ACS Appl. Mater. Interfaces* **2014**, *6*, 2185−2191.

(7) Xu, Y.-K.; Hwang, S.; Kim, S.; Chen, J.-Y. Two orders of magnitude fluorescence Enhancement of aluminum phthalocyanines by gold nanocubes: a remarkable improvement for cancer cell imaging and detection. *ACS Appl. Mater. Interfaces* **2014**, *6*, 5619−5628.

(8) Wei, W.; Lu, Y.; Chen, W.; Chen, S. One-pot synthesis, photoluminescence, and electrocatalytic properties of subnanometer-sized copper clusters. *J. Am. Chem. Soc.* **2011**, *133*, 2060−2063.

(9) Jia, X.; Li, J.; Wang, E. Cu nanoclusters with aggregation induced emission enhancement. *Small* **2013**, *9*, 3873−3879.

(10) Feng, J.; Ju, Y.; Liu, J.; Zhang, H.; Chen, X. Polyethyleneimine-templated copper nanoclusters via ascorbic acid reduction approach as ferric ion sensor. *Anal. Chim. Acta* **2015**, *854*, 153−160.

(11) Chen, J.; Ji, X.; Tinnefeld, P.; He, Z. Multifunctional dumbbell-shaped DNA-templated selective formation of fluorescent silver nanoclusters or copper nanoparticles for sensitive detection of biomolecules. *ACS Appl. Mater. Interfaces* **2016**, *8*, 1786−1794.

(12) Huang, H.; Li, H.; Wang, A.-J.; Zhong, S.-X.; Fang, K.-M.; Feng, J.-J. Green synthesis of peptide-templated fluorescent copper nanoclusters for temperature sensing and cellular imaging. *Analyst* **2014**, *139*, 6536−6541.

(13) Goswami, N.; Giri, A.; Bootharaju, M. S.; Xavier, P. L.; Pradeep, T.; Pal, S. K. Copper quantum clusters in protein matrix: potential sensor of Pb^{2+} ion. *Anal. Chem.* **2011**, *83*, 9676−9680.

(14) Kawasaki, H.; Hamaguchi, K.; Osaka, I.; Arakawa, R. ph-dependent synthesis of pepsin-mediated gold nanoclusters with blue green and red fluorescent emission. *Adv. Funct. Mater.* **2011**, *21*, 3508−3515.

(15) Karunasagar, D.; Arunachalam, J.; Gangadharan, S. Development of a 'collect and punch' cold vapour inductively coupled plasma mass spectrometric method for the direct determination of mercury at nanograms per litre levels. *J. Anal. At. Spectrom.* **1998**, *13*, 679−682.

(16) Cizdziel, J. V.; Gerstenberger, S. Determination of total mercury in human hair and animal fur by combustion atomic absorption spectrometry. *Talanta* **2004**, *64*, 918−921.

(17) Kim, H.-J.; Park, D.-S.; Hyun, M.-H.; Shim, Y.-B. Determination of HgII ion with a 1,11-Bis(8-quinoyloxy)-3,6,9-trioxaundecane-modified glassy carbon electrode using spin-coating technique. *Electroanalysis* **1998**, *10*, 303−306.

(18) Xu, X.; Thundat, T. G.; Brown, G. M.; Ji, H.-F. Detection of Hg^{2+} using microcantilever sensors. *Anal. Chem.* **2002**, *74*, 3611−3615.

(19) Khan, A.; Asiri, A. M.; Khan, A. A. P.; Rub, M. A.; Azum, N.; Rahman, M. M.; Khan, S. B.; Alamry, K. A.; Ghani, S. A. Sol-gel synthesis and characterization of conducting polythiophene/tin phosphate nano tetrapod composite cation-exchanger and its application as Hg(II) selective membrane electrode. *J. Sol-Gel Sci. Technol.* **2013**, *65*, 160−169.

(20) Chen, J.; Zhou, S.; Wen, J. Disposable strip biosensor for visual detection of Hg^{2+} based on Hg^{2+}-triggered toehold binding and exonuclease III-assisted signal amplification. *Anal. Chem.* **2014**, *86*, 3108−3114.

(21) Chen, J.-F.; Han, B.-B.; Ma, J.-F.; Liu, X.; Yang, Q.-Y.; Lin, Q.; Yao, H.; Zhang, Y.-M.; Wei, T.-B. Pillar[5]arene-based fluorescent polymer for selective detection and removal of mercury ions. *RSC Adv.* **2017**, *7*, 47709−47714.

(22) Hussain, M. M.; Rahman, M. M.; Arshad, M. N.; Asiri, A. M. Hg^{2+} sensor development based on (E)-N′-nitrobenzylidene-benzenesulfonohydrazide (NBBSH) derivatives fabricated on a glassy carbon electrode with a nafion matrix. *ACS Omega* **2017**, *2*, 420−431.

(23) Arshad, M. N.; Rahman, M. M.; Asiri, A. M.; Sobahi, T. R.; Yu, S.-H. Development of Hg^{2+} sensor based on N[prime or minute]-[1-(pyridin-2-yl)ethylidene]benzenesulfono-hydrazide (PEBSH) fabricated silver electrode for environmental remediation. *RSC Adv.* **2015**, *5*, 81275−81281.

(24) Wen, D.; Deng, L.; Guo, S.; Dong, S. Self-powered sensor for trace Hg^{2+} detection. *Anal. Chem.* **2011**, *83*, 3968−3972.

(25) Zhang, H.-L.; Li, W.-T.; Qu, W.-J.; Wei, T.-B.; Lin, Q.; Zhang, Y.-M.; Yao, H. Mercaptooxazole-phenazine based blue fluorescent sensor for the ultra-sensitive detection of mercury(ii) ions in aqueous solution. *RSC Adv.* **2017**, *7*, 47547−47551.

(26) Song, K. C.; Kim, J. S.; Park, S. M.; Chung, K.-C.; Ahn, S.; Chang, S.-K. Fluorogenic Hg^{2+}-selective chemodosimeter derived from 8-hydroxyquinoline. *Org. Lett.* **2006**, *8*, 3413−3416.

(27) Ikeda, M.; Matsu-ura, A.; Kuwahara, S.; Lee, S. S.; Habata, Y. Hg^{2+}-sensing system based on structures of complexes. *Org. Lett.* **2012**, *14*, 1564−1567.

(28) Li, T.; Dong, S.; Wang, E. Label-free colorimetric detection of aqueous mercury ion (Hg^{2+}) using Hg^{2+}-modulated G-quadruplex-based DNAzymes. *Anal. Chem.* **2009**, *81*, 2144−2149.

(29) Lin, Q.; Mao, P.-P.; Fan, Y.-Q.; Liu, L.; Liu, J.; Zhang, Y.-M.; Yao, H.; Wei, T.-B. A novel supramolecular polymer gel based on naphthalimide functionalized-pillar[5]arene for the fluorescence detection of Hg^{2+} and I^- and recyclable removal of Hg^{2+} via cation-[small pi] interactions. *Soft Matter* **2017**, *13*, 7085−7089.

(30) Chang, H.-C.; Chang, Y.-F.; Fan, N.-C.; Ho, J.-a. A. Facile preparation of high-quantum-yield gold nanoclusters: application to probing mercuric ions and biothiols. *ACS Appl. Mater. Interfaces* **2014**, *6*, 18824−18831.

(31) Lu, W.; Qin, X.; Liu, S.; Chang, G.; Zhang, Y.; Luo, Y.; Asiri, A. M.; Al-Youbi, A. O.; Sun, X. Economical, green synthesis of fluorescent carbon nanoparticles and their use as probes for sensitive and selective detection of mercury (II) ions. *Anal. Chem.* **2012**, *84*, 5351−5357.

(32) Hu, X.; Wang, W.; Huang, Y. Copper nanocluster-based fluorescent probe for sensitive and selective detection of Hg^{2+} in water and food stuff. *Talanta* **2016**, *154*, 409−415.

(33) Awual, M. R.; Hasan, M. M.; Eldesoky, G. E.; Khaleque, M. A.; Rahman, M. M.; Naushad, M. Facile mercury detection and removal from aqueous media involving ligand impregnated conjugate nanomaterials. *Chem. Eng. J.* **2016**, *290*, 243−251.

(34) Li, X.; Zhu, S.; Xu, B.; Ma, K.; Zhang, J.; Yang, B.; Tian, W. Self-assembled graphene quantum dots induced by cytochrome c: a novel

DOI: 10.1021/acsomega.7b01052
ACS Omega 2017, 2, 9109−9117

biosensor for trypsin with remarkable fluorescence enhancement. *Nanoscale* **2013**, *5*, 7776−7779.
(35) Guo, C.; Irudayaraj, J. Fluorescent Ag clusters via a protein-directed approach as a Hg(II) ion sensor. *Anal. Chem.* **2011**, *83*, 2883−2889.
(36) Jiang, H.; Zhang, Y.; Wang, X. Single cytidine units-templated syntheses of multi-colored water-soluble Au nanoclusters. *Nanoscale* **2014**, *6*, 10355−10362.
(37) Lisiecki, I.; Pileni, M. Copper metallic particles synthesized "in situ" in reverse micelles: influence of various parameters on the size of the particles. *J. Phys. Chem.* **1995**, *99*, 5077−5082.
(38) Mott, D.; Galkowski, J.; Wang, L.; Luo, J.; Zhong, C.-J. Synthesis of size-controlled and shaped copper nanoparticles. *Langmuir* **2007**, *23*, 5740−5745.
(39) Shichibu, Y.; Negishi, Y.; Tsunoyama, H.; Kanehara, M.; Teranishi, T.; Tsukuda, T. Extremely high stability of glutathionate-protected Au25 clusters against core etching. *Small* **2007**, *3*, 835−839.
(40) Qiao, Y.; Xu, T.; Zhang, Y.; Zhang, C.; Shi, L.; Zhang, G.; Shuang, S.; Dong, C. Green synthesis of fluorescent copper nanoclusters for reversible pH-sensors. *Sens. Actuators, B* **2015**, *220*, 1064−1069.
(41) Miao, H.; Zhong, D.; Zhou, Z.; Yang, X. Papain-templated Cu nanoclusters: assaying and exhibiting dramatic antibacterial activity cooperating with H_2O_2. *Nanoscale* **2015**, *7*, 19066−19072.
(42) Ghosh, S.; Anand, U.; Mukherjee, S. Luminescent silver nanoclusters acting as a label-free photoswitch in metal ion sensing. *Anal. Chem.* **2014**, *86*, 3188−3194.
(43) Wang, C.; Wang, C.; Xu, L.; Cheng, H.; Lin, Q.; Zhang, C. Protein-directed synthesis of pH-responsive red fluorescent copper nanoclusters and their applications in cellular imaging and catalysis. *Nanoscale* **2014**, *6*, 1775−1781.
(44) Xie, J.; Zheng, Y.; Ying, J. Y. Protein-directed synthesis of highly fluorescent gold nanoclusters. *J. Am. Chem. Soc.* **2009**, *131*, 888−889.
(45) Barth, A. Infrared spectroscopy of proteins. *Biochim. Biophys. Acta, Bioenerg.* **2007**, *1767*, 1073−1101.
(46) Chaudhari, K.; Xavier, P. L.; Pradeep, T. Understanding the evolution of luminescent gold quantum clusters in protein templates. *ACS Nano* **2011**, *5*, 8816−8827.
(47) Koski, K. J.; Cha, J. J.; Reed, B. W.; Wessells, C. D.; Kong, D.; Cui, Y. High-density chemical intercalation of zero-valent copper into Bi_2Se_3 nanoribbons. *J. Am. Chem. Soc.* **2012**, *134*, 7584−7587.
(48) Ghosh, R.; Sahoo, A. K.; Ghosh, S. S.; Paul, A.; Chattopadhyay, A. Blue-emitting copper nanoclusters synthesized in the presence of lysozyme as candidates for cell labeling. *ACS Appl. Mater. Interfaces* **2014**, *6*, 3822−3828.
(49) Zhang, R.; Chen, W. Nitrogen-doped carbon quantum dots: Facile synthesis and application as a "turn-off" fluorescent probe for detection of Hg^{2+} ions. *Biosens. Bioelectron.* **2014**, *55*, 83−90.
(50) Kawasaki, H.; Yoshimura, K.; Hamaguchi, K.; Arakawa, R. Trypsin-stabilized fluorescent gold nanocluster for sensitive and selective Hg^{2+} detection. *Anal. Sci.* **2011**, *27*, 591.
(51) Zang, J.; Li, C.; Zhou, K.; Dong, H.; Chen, B.; Wang, F.; Zhao, G. Nanomolar Hg^{2+} detection using β-lactoglobulin-stabilized fluorescent gold nanoclusters in beverage and biological media. *Anal. Chem.* **2016**, *88*, 10275−10283.
(52) Zheng, B.; Zheng, J.; Yu, T.; Sang, A.; Du, J.; Guo, Y.; Xiao, D.; Choi, M. M. F. Fast microwave-assisted synthesis of AuAg bimetallic nanoclusters with strong yellow emission and their response to mercury(II) ions. *Sens. Actuators, B* **2015**, *221*, 386−392.
(53) Deng, L.; Zhou, Z.; Li, J.; Li, T.; Dong, S. Fluorescent silver nanoclusters in hybridized DNA duplexes for the turn-on detection of Hg^{2+} ions. *Chem. Commun.* **2011**, *47*, 11065−11067.
(54) Guo, W.; Yuan, J.; Wang, E. Oligonucleotide-stabilized Ag nanoclusters as novel fluorescence probes for the highly selective and sensitive detection of the Hg^{2+} ion. *Chem. Commun.* **2009**, 3395−3397.
(55) Lan, G.-Y.; Chen, W.-Y.; Chang, H.-T. Control of synthesis and optical properties of DNA templated silver nanoclusters by varying DNA length and sequence. *RSC Adv.* **2011**, *1*, 802−807.
(56) Morishita, K.; MacLean, J. L.; Liu, B.; Jiang, H.; Liu, J. Correlation of photobleaching, oxidation and metal induced fluorescence quenching of DNA-templated silver nanoclusters. *Nanoscale* **2013**, *5*, 2840−2849.
(57) Guo, Y.; Wang, Z.; Shao, H.; Jiang, X. Hydrothermal synthesis of highly fluorescent carbon nanoparticles from sodium citrate and their use for the detection of mercury ions. *Carbon* **2013**, *52*, 583−589.
(58) Liu, J.; Chen, Y.; Wang, W.; Feng, J.; Peng, S.; Ma, S.; Chen, H.; Chen, X. Effective synthesis of highly fluorescent nitrogen doped carbon nanoparticles for selective sensing of Hg^{2+} in food and cosmetics samples. *RSC Adv.* **2016**, *6*, 89916−89924.
(59) Huang, C.-C.; Yang, Z.; Lee, K.-H.; Chang, H.-T. Synthesis of highly fluorescent gold nanoparticles for sensing mercury(II). *Angew. Chem.* **2007**, *119*, 6948−6952.
(60) Klein, G.; Kaufmann, D.; Schurch, S.; Reymond, J.-L. A fluorescent metal sensor based on macrocyclic chelation. *Chem. Commun.* **2001**, 561−562.
(61) Feng, J.; Chen, Y.; Han, Y.; Liu, J.; Ren, C.; Chen, X. Fluorescent carbon nanoparticles: A low-temperature trypsin-assisted preparation and Fe^{3+} sensing. *Anal. Chim. Acta* **2016**, *926*, 107−117.
(62) Liu, Y.; Gong, X.; Gao, Y.; Song, S.; Wu, X.; Shuang, S.; Dong, C. Carbon-based dots co-doped with nitrogen and sulfur for Cr(vi) sensing and bioimaging. *RSC Adv.* **2016**, *6*, 28477−28483.

DOI: 10.1021/acsomega.7b01052
ACS Omega 2017, 2, 9109−9117